

Thermal Degradation Kinetics of Epoxy/Organically Modified Montmorillonite Nanocomposites

Ivan Brnardić, Jelena Macan, Hrvoje Ivanković, Marica Ivanković

Faculty of Chemical Engineering and Technology, University of Zagreb, Marulićev trg 19, HR-10001 Zagreb, Croatia

Received 4 May 2007; accepted 1 August 2007

DOI 10.1002/app.27230

Published online 29 October 2007 in Wiley InterScience (www.interscience.wiley.com).

ABSTRACT: Nanocomposites based on a commercial epoxy resin and organically modified montmorillonites (OMMTs), containing 5 and 10 phr OMMT, were prepared and characterized. Poly(oxypropylene) diamine (Jeffamine D400) and octadecylamine were used as organic modifiers. Another poly(oxypropylene) diamine (Jeffamine D230) was used as a curing agent. The thermal degradation kinetics of the neat resin system and nanocomposites were investigated by thermogravimetric analysis. The dispersion of silicate layers within the crosslinked epoxy matrix was verified by transmission electron microscopy. The activation

energy of degradation for the investigated systems was determined by the isoconversional Kissinger–Akahira–Sunose method. The thermal behavior of the neat resin systems and nanocomposites was modeled with an empirical kinetic model. The influence of organic modifiers and the OMMT loading on the thermal stability of the nanocomposites was discussed. © 2007 Wiley Periodicals, Inc. *J Appl Polym Sci* 107: 1932–1938, 2008

Key words: degradation; nanocomposites; organoclay; thermogravimetric analysis (TGA); thermosets

INTRODUCTION

In the last decade, organically modified layered silicates have become recognized as useful fillers in polymer-matrix composites. The morphology of the nanocomposites can evolve from so-called intercalated nanocomposites, in which a regular alternation of the layered silicates and polymer monolayers can be observed, to the exfoliated (delaminated) type of nanocomposites, in which individual nanometer-thick silicate layers are randomly and homogeneously distributed throughout the polymer matrix. The nanoscopic distribution of the platelets in a polymer can lead to greatly improved mechanical, thermal, and gas-barrier properties.

Epoxy resins are widely used as polymer matrices for composites. To date, epoxy-layered silicate nanocomposites have gained widespread attention with respect to their synthesis, morphology, and properties.^{1–18} However, in very few studies^{2,14,18–21} has their thermal stability at elevated temperatures been investigated.

In this work, the thermal degradation kinetics of nanocomposites based on organically modified montmorillonite (OMMT) and a commercial epoxy

resin were studied. These composite materials were previously characterized, and their cure kinetics were studied.^{22,23}

EXPERIMENTAL

An epoxy resin, diglycidyl ether of bisphenol A (DGEBA; DER 331), with an epoxy equivalent weight of 187 g/mol was obtained from Dow Chemicals (Midland, MI). Poly(oxypropylene) diamine, provided under the trade name Jeffamine D230 by Fluka (Buchs, Switzerland), with an N–H equivalent weight of 57.5 g/mol, was used as a curing agent. The clay was a Wyoming-type montmorillonite provided by M. I. Drilling Fluids Co. (Porra Quay, Alberdeen, Scotland) Octadecylamine, provided by Kemika (Zagreb, Croatia), and poly(oxypropylene) diamine (Jeffamine D400), provided by Fluka, were used as modifiers for montmorillonite. The materials were used as received. OMMTs were prepared as described previously.^{22,23}

To prepare the neat epoxy resin system, DGEBA and a stoichiometric amount of Jeffamine D230 were mixed and stirred at room temperature in a closed vessel for 60 min. To prepare the nanocomposite systems, epoxy resin was mixed with desired amounts of OMMTs (5 and 10 g of OMMT per 100 g of epoxy) at 75°C for 24 h and sonicated for 15 min. Samples were designated according to the organic modifier of montmorillonite and OMMT loading: O_MMT_5 and O_MMT_10 for nanocomposites with 5 and 10 phr octadecylamine modified montmorillonite and J_MMT_5 and J_MMT_10 for nanocompo-

Correspondence to: M. Ivanković (mivank@fkit.hr).

Contract grant sponsor: Ministry of Science, Education, and Sport of the Republic of Croatia (as part of the research project “Bioceramic, Polymer, and Composite Nanostructured Materials”); contract grant number: 125-1252970-3005.

Journal of Applied Polymer Science, Vol. 107, 1932–1938 (2008)
© 2007 Wiley Periodicals, Inc.

sites with 5 and 10 phr poly(oxypropylene) diamine (Jeffamine D400) modified montmorillonite, respectively. After the mixture was cooled to room temperature, a stoichiometric amount of the curing agent Jeffamine D230 was added with thorough mixing for 60 min. The mixtures were poured into molds and cured at 80°C for 3 h, and this was followed by post-curing at 120°C for 1 h.

The materials were investigated by means of X-ray diffraction (XRD), as reported previously.^{22,23} The initial *d*-spacing of the OMMTs was determined to be 21.9 Å for octadecylamine-modified montmorillonite and 16.3 Å for poly(oxypropylene) diamine modified montmorillonite. In all composite systems, the absence of basal spacing (001) was observed. It is common practice to classify a nanocomposite as fully exfoliated from the absence of the (001) reflection. However, disordered layers (bunched together but not parallel stacked) are not detected by XRD. Thus, a silent XRD may hide a large number of disordered tactoids and can be highly misleading when employed as a single tool for quantifying a nanocomposite structure or filler dispersion. To verify the morphology of the cured epoxy resin/OMMT composites, the materials were investigated by means of transmission electron microscopy (TEM) with a JEOL 200 CX microscope (Tokyo, Japan) with a 120-kV acceleration voltage.

The weight loss of fully cured samples, weighing approximately 15 mg, was measured by thermogravimetric analysis (TGA) with a PerkinElmer TGS-2 thermobalance (Norwalk, CT). The samples were heated from room temperature to 1000°C at four different heating rates (5, 10, 15, and 20°C/min) in a nitrogen gas flow of 150 cm³/min.

RESULTS AND DISCUSSION

Degradation behavior

Examples of TGA curves obtained from the neat resin system and nanocomposites containing 5 and 10 g of OMMT per 100 g of epoxy resin, under a nitrogen atmosphere, are shown in Figure 1. The temperature at the maximum rate of weight loss was determined from the first derivative of the TGA curves (Figs. 2 and 3) and is summarized in Table I. In comparison with the neat resin system, an almost identical or slightly decreased onset temperature of degradation for the nanocomposites was observed (Table I). The shift was most pronounced in the nanocomposite O_MMT_10. Similar findings for an onset temperature decrease are reported in the literature.^{20,21} As shown by the TGA and derivative thermogravimetry (DTG) curves in Figure 4(a,b), the thermal decomposition of organic modifiers in neat OMMTs started at lower temperatures (at about

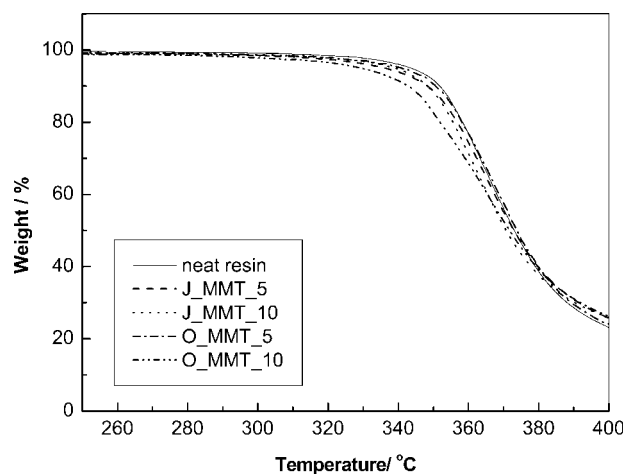


Figure 1 TGA curves of the investigated systems obtained at a heating rate of 5°C/min.

200°C) in comparison with the neat resin. Because of this, the addition of nanofillers could accelerate the thermodegradation process in the nanocomposites with respect to that of the neat resin. DTG curves of the neat resin system and nanocomposites with J_MMT have similar shapes (Fig. 2), indicating a single-step degradation process. The reason that a separate degradation of the interlayer exchanged ions was not observed could be a very low concentration of organic ions in the system. A shoulder on the DTG peak of the nanocomposites with O_MMT indicates two main steps of the degradation process (Fig. 3). The shoulder is more pronounced for the nanocomposites with higher O_MMT loadings (10 phr) and lower heating rates.

Isoconversional kinetic analysis

To describe the degradation of the investigated systems, the isoconversional kinetic analysis of TGA curves was performed first. As is known, isoconversional methods do not assume a kinetic model [$f(\alpha)$] to calculate the activation energy of a reaction but instead calculate an apparent activation energy (E_a) directly from the TGA curves. As a result, a functional dependence of E_a on conversion (α) is obtained, which can indicate the complexity of the reaction mechanism.

Integral isoconversional methods, such as the Flynn–Wall–Ozawa^{24,25} and Kissinger–Akahira–Sunose (KAS) methods,^{26,27} are suited to the analysis of TGA curves because they do not require the experimental data to be differentiated beforehand.²⁸ As the two integral methods are mathematically equivalent,²⁹ the KAS equation was chosen because it was shown to be correct for a wider interval of activation energies:³⁰

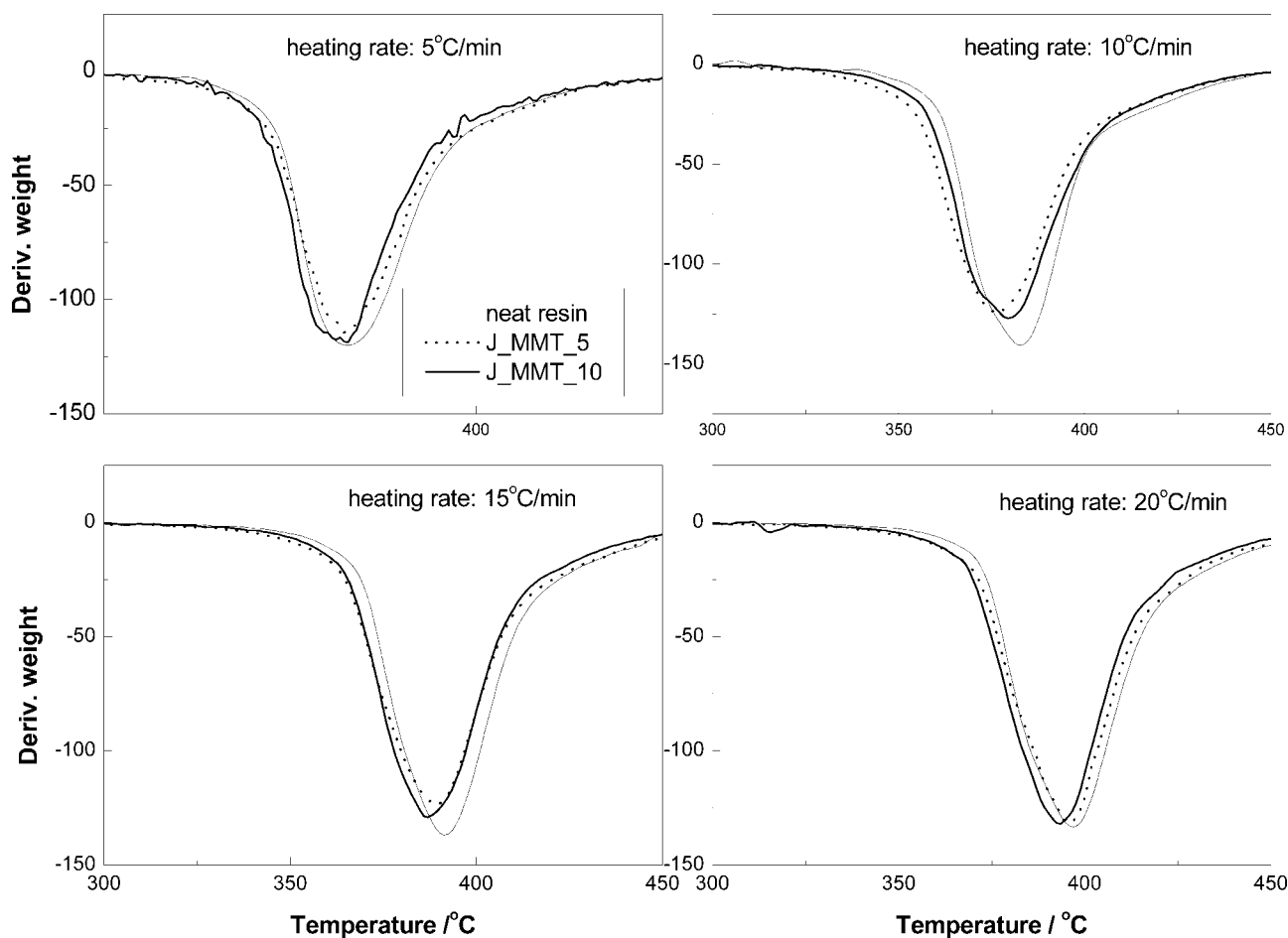


Figure 2 DTG curves of J_MMT systems versus the epoxy neat resin system at four different heating rates.

$$\ln \left(\frac{\beta}{T^2} \right) = [\ln(k_0 R / E_a) - \ln G(\alpha)] - \frac{E_a}{RT} \quad (1)$$

where β is the heating rate, T is the thermodynamic temperature, k_0 is the pre-exponential factor, R is the general gas constant ($8.314 \text{ J mol}^{-1} \text{ K}^{-1}$), and $G(\alpha)$ is the integral form of kinetic model $f(\alpha)$.

α was calculated as follows:

$$\frac{\alpha(T) = m_0 - m(T)}{m_0 - m_\infty} \quad (2)$$

where m_0 is the initial sample mass, $m(T)$ is the sample mass at temperature T and m_∞ is the final sample mass. The initial loss of mass at temperatures under 200°C , which was ascribed to the evaporation of adsorbed moisture, was disregarded.

From isoconversional plots of $\ln(\beta/T^2)$ versus $1/T$, for values of α in the 0.05–0.90 range, the activation energy was calculated, as illustrated in Figure 5, for the neat epoxy/Jeffamine D230 system. The dependence of E_a on α is presented in Figure 6, indicating the change in the degradation mechanisms in the investigated α (or temperature) range. The reason for the significant increase in E_a at higher α values (>0.6)

could be a shift from chemically controlled kinetics to diffusion-controlled kinetics. It is also evident that the activation energy is dependent on the OMMT loading. The highest activation energies were obtained for nanocomposite systems with 5 phr OMMTs. The activation energy calculated for nanocomposite systems with 10 phr OMMTs was comparable to or even lower than E_a of neat resin system (see O_MMT_10, $\alpha < 0.4$, in Fig. 6). All these findings were expected from the results discussed earlier. An activation energy decrease when the OMMT loading is higher than 6 phr has been reported in the literature.¹⁹ The finding was explained by different degrees of intercalation/exfoliation of the layered silicate in the polymer matrix with different OMMT loadings. It was supposed that at a relatively low OMMT loading (<8 phr), the nanocomposite developed an exfoliation-dominant structure. When the OMMT loading increased further, the nanocomposites developed an exfoliated/intercalated structure. As the tactoids were less effective in blocking heat and the diffusion of volatile decomposition products out of the material than the exfoliated platelets, the activation energy started to decrease with the OMMT loading.

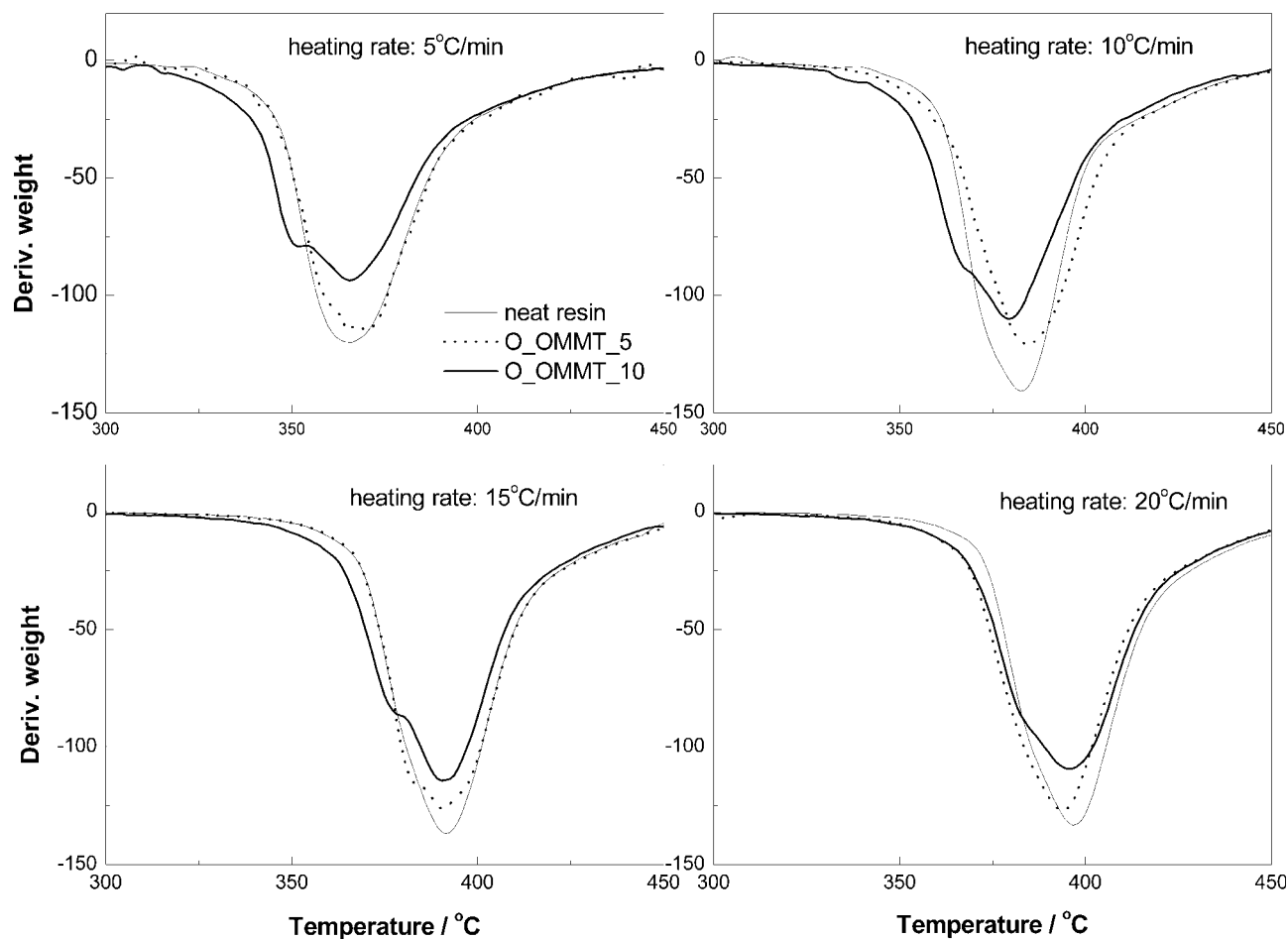


Figure 3 DTG curves of O_MMT systems versus the epoxy neat resin system at four different heating rates.

TABLE I
Thermal Stability Parameters of the Investigated Systems: Onset Temperature of Degradation (T_{on}), Temperature of Maximal Degradation Rate (T_{max}), and IPDT

System	Heating rate (°C/min)	T_{on} (°C)	T_{max} (°C)	IPDT (°C)
Neat resin	5	351	365	497
	10	367	383	
	15	375	391	
	20	379	397	
J_MMT_5	5	351	370	519
	10	363	376	
	15	369	389	
	20	380	396	
J_MMT_10	5	349	364	554
	10	365	379	
	15	372	387	
	20	377	393	
O_MMT_5	5	351	368	514
	10	368	385	
	15	373	390	
	20	376	393	
O_MMT_10	5	344	366	541
	10	358	379	
	15	369	390	
	20	376	395	

TEM images of systems O_MMT_5 and J_MMT_5 are shown in Figure 7(a,b), indicating a heterogeneous structure, that is, a coexistence of tactoids and intercalated and exfoliated layers. The extended dark areas in the TEM images are projections of layers parallel or oblique to the sample surface. In the O_MMT_5 system [Fig. 7(a)], O_MMT layers were inhomogeneously distributed, and large regions of pure epoxy matrix were observed. J_MMT layers [Fig. 7(b)] seemed to be distributed much more homogeneously in the matrix. This may be a reason that the J_MMT_5 system showed higher activation energy for degradation in comparison with O_MMT_5.

Modeling of the degradation kinetics

A goal of kinetic analysis is to simulate the thermal behavior of a material. The degradation of polymer materials often proceeds via a complex mechanism, and elucidating the kinetics for overlapping reactions is a very demanding procedure. If the degradation is studied to ascertain the processing parameters and appropriate working conditions for the material, the use of simple empirical models (with an average

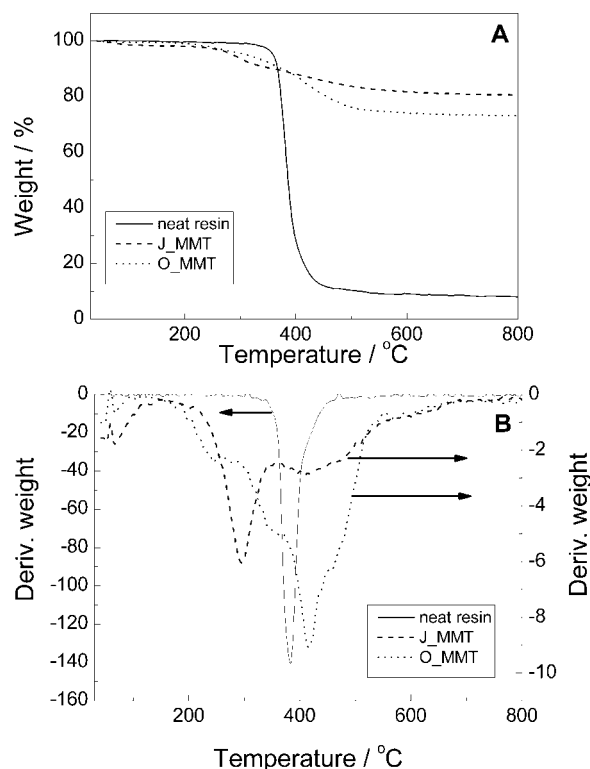


Figure 4 (A) TGA and (B) DTG curves of the neat OMMTs versus the neat epoxy resin system.

value of the activation energy) in kinetic analysis is justified.³¹ In this work, an autocatalytic model of reaction was chosen:

$$\frac{d\alpha}{dt} = k_0 \exp(-E_a/RT) \alpha^m (1 - \alpha)^n \quad (3)$$

where $d\alpha/dt$ is the rate of reaction and m and n are empirical coefficients. The model was fitted simultaneously to experimental datasets obtained at differ-

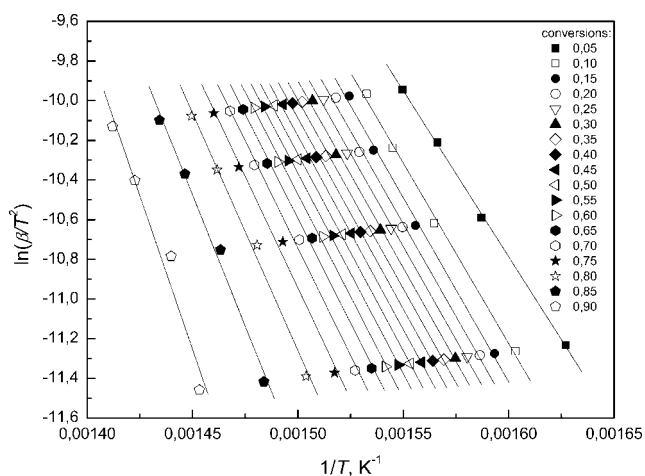


Figure 5 Isoconversional plots used to calculate the activation energy at the listed conversions by the KAS method for the neat resin system.

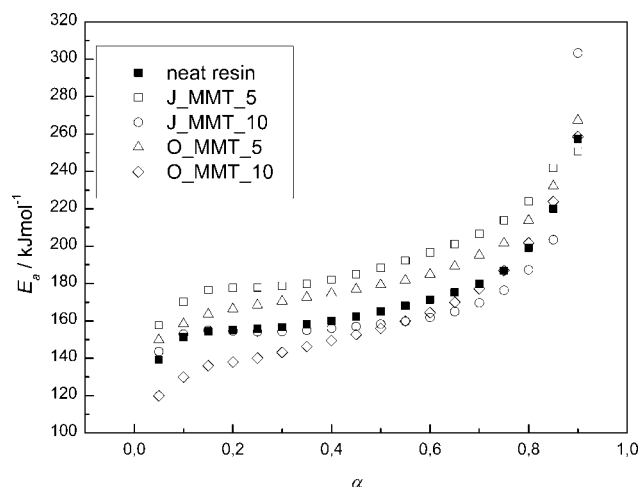


Figure 6 Dependence of E_a on α as obtained by the KAS method for all investigated systems.

ent heating rates with the program Wolfram Mathematica 5.0. The model parameters were optimized by minimization of the mean square difference between the calculated and experimental conversions. The average values of the apparent activation energy obtained by the KAS method ($E_{a,KAS}$) in the conversion interval between 0.15 and 0.75 were used as initial values and, if necessary, were modified to

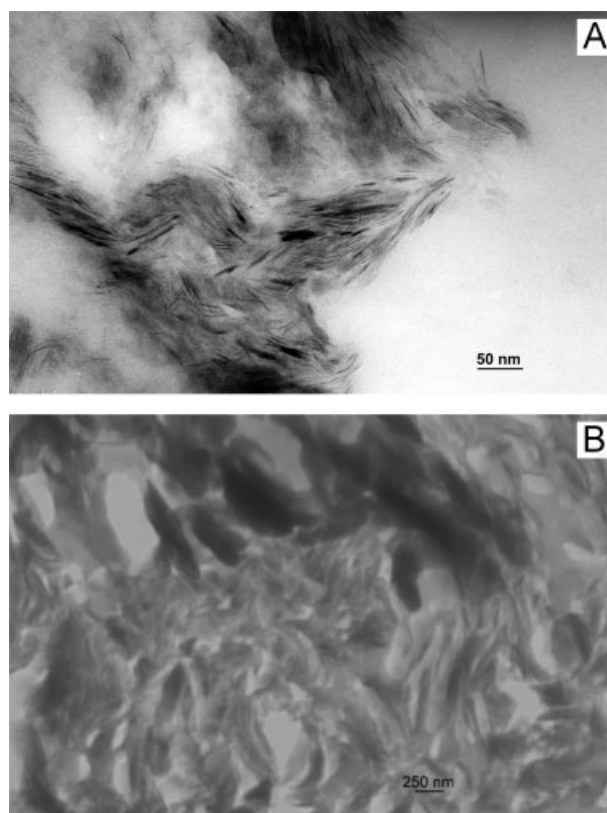


Figure 7 TEM images of the investigated systems: (A) O_MMT_5 and (B) J_MMT_5.

TABLE II
 E_a , k_0 , and Empirical Exponents m and n for the Given Systems and Model [Eq. (3)]

System	$E_{a,fit}$ (kJ/mol)	$E_{a,KAS}$ (kJ/mol)	k_0 (s^{-1})	m	n
Neat resin	179	165	exp(28.8)	0.55	1.90
J_MMT_5	197	189	exp(32.5)	0.60	2.08
J_MMT_10	173	160	exp(28.1)	0.65	1.99
O_MMT_5	214	179	exp(35.3)	0.52	2.15
O_MMT_10	177	155	exp(28.3)	0.42	1.76

obtain the most satisfying fit. The model parameters are summarized in Table II. As shown in Figure 8, the chosen model predicted the conversion profiles fairly well. Because in modeling an average E_a value was used that was lower than E_a for the final steps of degradation (see Fig. 6 and Table II), the model predicted an earlier end of the degradation process (at lower temperatures).

Thermal stability

It is difficult to compare the thermal stability of investigated materials solely from the results of ki-

netic modeling. Because of this, another parameter, the integral procedure degradation temperature (IPDT), was determined as well (see Table I). IPDT takes into account the whole degradation process¹⁹ and represents the inherent thermal stability of a material. As seen, the IPDT of the nanocomposites was higher than the IPDT of the neat resin system. The nanocomposites with octadecylamine-modified montmorillonite had higher thermal stability than the nanocomposites containing poly(oxypropylene) diamine modified montmorillonite. A trend of reduced weight loss (or improved char formation) was observed with OMMT addition as well. As char acts as an insulator and mass-transport barrier for volatile degradation products,³² the presence of silicate layers in the epoxy matrix can reduce or prevail over the negative influence of interlayer organic ions on the thermal stability of the investigated materials.

CONCLUSIONS

TGA was used to study the kinetics of the thermal degradation of nanocomposites based on epoxy resin

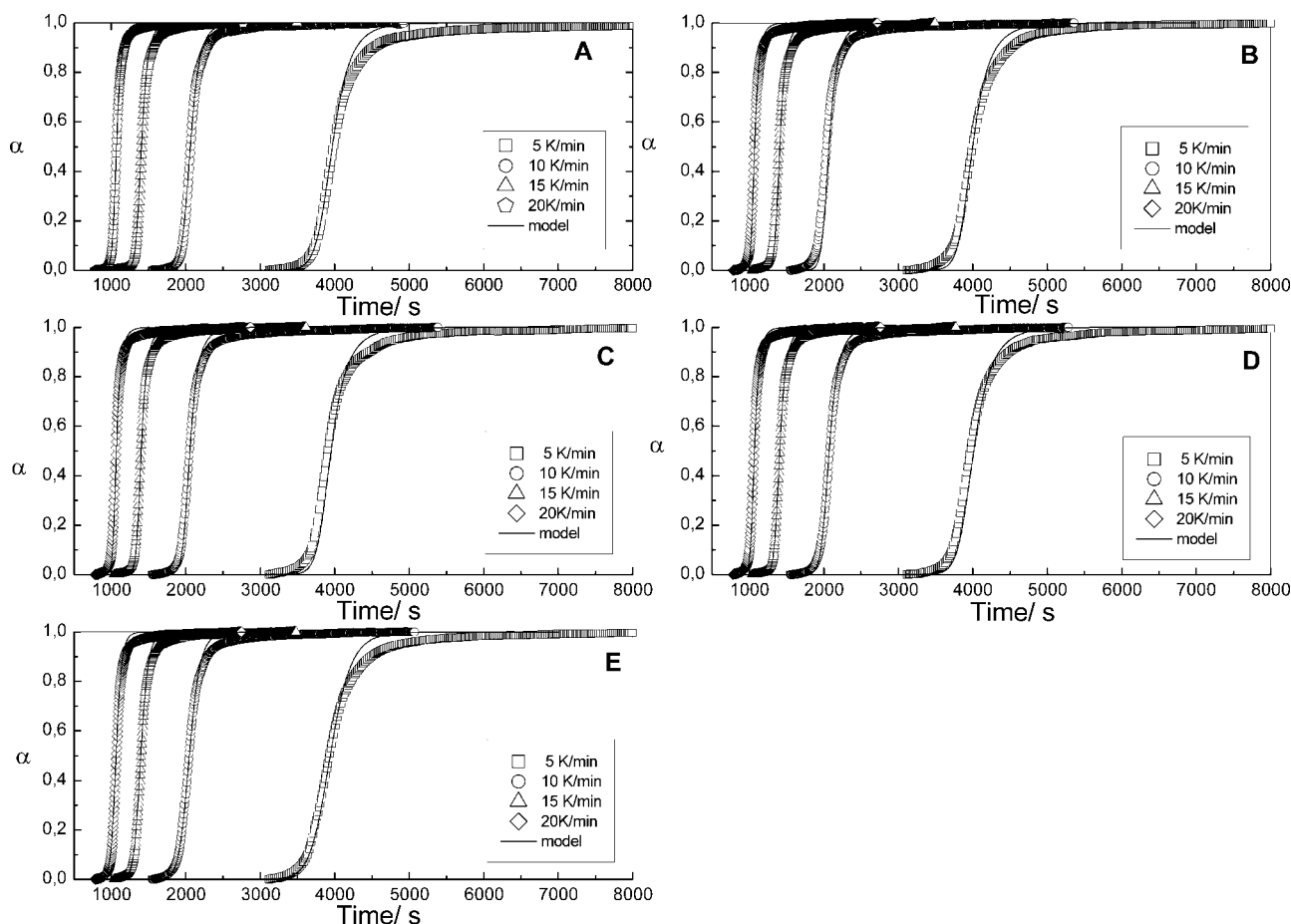


Figure 8 Comparison of (· · ·) experimental data with (—) the kinetic model data for all investigated systems: (A) neat resin, (B) J_MMT_5, (C) J_MMT_10, (D) O_MMT_5, and (E) O_MMT_10. Zero time corresponds to the temperature of 40°C (313 K).

and OMMTs. Interlayer organic ions in OMMTs were more prone to degradation than the neat epoxy resin system and caused a slight decrease in the onset temperature of thermal degradation in the nanocomposites. E_a for the degradation process was calculated with the isoconversional KAS method, and the kinetics were described with an empirical autocatalytic model. Nanocomposites with 5 phr OMMT had the highest values of E_a , which indicated a higher degree of exfoliation of silicate layers in the epoxy matrix in comparison with the nanocomposites with 10 phr OMMT. The IPDT and final char content increased with increasing OMMT loading. Despite the observed differences, it is fair to say that very little change in the thermal stability of the nanocomposites with respect to that of the neat resin was in fact observed.

References

1. Wang, M. S.; Pinnavaia, T. J. *Chem Mater* 1994, 6, 468.
2. Messersmith, P. B.; Giannelis, E. P. *Chem Mater* 1994, 6, 1719.
3. Lan, T.; Pinnavaia, T. J. *Chem Mater* 1994, 6, 2216.
4. Lan, T.; Kaviratna, P. D.; Pinnavaia, T. J. *Chem Mater* 1995, 7, 2144.
5. Lan, T.; Kaviratna, P. D.; Pinnavaia, T. J. *J Phys Chem Solids* 1996, 57, 1005.
6. Brown, J. M.; Curliss, D.; Vaia, R. A. *Chem Mater* 2000, 12, 3376.
7. Lu, J. K.; Ke, Y. C.; Qi, Z. N.; Yi, X. S. *J Polym Sci Part B: Polym Phys* 2001, 39, 115.
8. Kornmann, X.; Lindberg, H.; Berglund, L. A. *Polymer* 2001, 42, 1303.
9. Kornmann, X.; Lindberg, H.; Berglund, L. A. *Polymer* 2001, 42, 4493.
10. Chin, I. J.; Thurn-Albrecht, T.; Kim, H. C.; Russel, T. P.; Wang, J. *Polymer* 2001, 42, 5947.
11. Butzloff, P.; D'souza, N. A.; Golden, T. D.; Garrett, D. *Polym Eng Sci* 2001, 41, 1794.
12. Chen, K. H.; Yang, S. M. *J Appl Polym Sci* 2002, 86, 414.
13. Suh, D. J.; Park, O. O. *J Appl Polym Sci* 2002, 83, 2143.
14. Park, S. J.; Seo, D. I.; Lee, J. R. *J Colloid Interface Sci* 2002, 251, 160.
15. Triantafillidis, C. S.; LeBaron, P. C.; Pinnavaia, T. J. *J Solid State Chem* 2002, 167, 354.
16. Salahuddin, N.; Moet, A.; Hiltner, A.; Baer, E. *Eur Polym J* 2002, 38, 1477.
17. Xu, W. B.; Bao, S. P.; Shen, S. J.; Hang, G. P.; He, P. S. *J Appl Polym Sci* 2003, 88, 2932.
18. Salahuddin, N. *Polym Adv Technol* 2004, 15, 251.
19. Guo, B. C.; Jia, D. M.; Cai, C. G. *Eur Polym J* 2004, 40, 1743.
20. Gu, A. J.; Liang, G. Z. *Polym Degrad Stab* 2003, 80, 383.
21. Becker, O.; Varley, R. J.; Simon, G. P. *Eur Polym J* 2004, 40, 187.
22. Ivanković M.; Brnardić I.; Ivanković H.; Mencer, H. J. *J Appl Polym Sci* 2006, 99, 550.
23. Brnardić I.; Ivanković M.; Ivanković H.; Mencer, H. J. *J Appl Polym Sci* 2006, 100, 1765.
24. Ozawa, T. *Bull Chem Soc Jpn* 1965, 38, 1881.
25. Flynn, J. H.; Wall, L. A. *J Polym Sci Polym Lett Ed* 1966, 4, 323.
26. Kissinger, H. E. *Anal Chem* 1957, 29, 1702.
27. Akahira, T.; Sunose, T. *Res Rep Chiba Inst Technol* 1971, 16, 22.
28. Vyazovkin, S. *Thermochim Acta* 2000, 355, 155.
29. Graydon, J. W.; Thorpe, S. J.; Kirk, D. W. *Acta Metall Mater* 1994, 42, 3163.
30. Gao, Z. M.; Nakada, M.; Amasaki, I. *Thermochim Acta* 2001, 369, 137.
31. Torre, L.; Kenny, J. M.; Maffezzoli, A. M. *J Mater Sci* 1998, 33, 3137.
32. Gilman, J. W. *J Appl Clay Sci* 1999, 15, 31.